# 1EVALUATION OF GEOTHERMAL RESOURCES IN A HOTSPOT REALM: MAURITIUS ISLAND (INDIAN OCEAN)

**C. Pasqua[1,2], M. Verdoya[2], P. Chiozzi[2], L. Marini[1]**
[1] ELC-Electroconsult, Via Marostica, 1, 20146 Milano, Italy
[2]DISTAV, University of Genova, Italy
claudio.pasqua@elc-electroconsult.com

**ABSTRACT**

Geochemical and geothermal investigations were performed in the Mauritius Island, located along the Seychelles-Mascarene Plateau, aimed at the preliminary assessment of possible geothermal resources. The central part of the island may be the most suitable as characterized by the most recent volcanic activity (0.03 Ma). Geochemical analyses of water samples collected from this area indicate no mature water and the chemical features are ascribable to short-term water-rock interaction in shallow hydrogeological circuits. A gradient borehole was drilled and thermal logs performed after complete thermal equilibration to evaluate the thermal gradient in central part of the island. A value of 43 °C $km^{-1}$ was measured and a similar result was obtained by logging a deep well no longer used for water extraction. The results point to a weak or null deep-seated thermal anomaly beneath Mauritius. This might mean that the deep thermal processes (mantle plume) invoked to occur in the hotspot area do not likely yield any particular thermal signature.

## 1. INTRODUCTION

The Island of Mauritius is the emerging portion of a huge submarine, aseismic, volcanic plateau, which is part of the Africa plate and extends in the SW part of the Indian Ocean. The plateau is related to a long-lived Réunion hotspot track, whose present-day expression is the active volcano of La Réunion Island, located about 200 km SW of Mauritius (Fig. 1).
The Réunion hotspot is part of the Chagos-Laccadive Ridge, emerging south of the Deccan Traps flood basalt province in western India and continuing south-westwards to the Mascarene archipelago, in the Indian Ocean (see e.g. Duncan and Richards, 1991). The northern part of the plateau includes the Seychelles Bank, whose continental nature is well recognized (e.g. Hammond et al., 2012). The plateau include also the banks of Saya de Malha and Nazareth, which lie on oceanic crust, are very shallow (a few tens of meters deep) and bounded by steep scarps that comprise an arc extending for about 2000 km. To the south, a large central volcano rising 5000 m above the seafloor and culminating 800 m above sea level constitutes Mauritius, the second largest island of the Mascarene archipelago. La Réunion Island, 170 km SW from Mauritius, has no topographic continuity with the swell and consists of a broad elliptic volcanic shield with a major axis reaching 200 km at seafloor level and a height of more than 7000 m above the oceanic floor.
The two islands are bounded by two fracture zones, Mahanoro to the west and Mauritius to the east. An extinct spreading centre (ocean paleo-rift), located south-west of the plateau, in the central part of the Mascarene Basin (60-90 Ma), is another natural boundary. The plateau and the fracture zones separate the Mascarene Basin from the Madagascar Basin (66-45 Ma) in the southeast, which was created by the spreading of the Central Indian Ridge.
The hotspot track is characterised by age-progressive volcanic centres which have migrated from north to south since 65 Ma ago to the Present (see Fig. 1). The hotspot activity has affected an old (40-90 Ma; Müller et al., 2008) and thick lithosphere. Dating of basalts from ODP site 707 (Duncan et al., 1989) indicates that the saddle between Seychelles and Saya de Malha Banks is 64 Ma old and this region erupted at about the time when seafloor spreading along the nascent northern section of the central Indian Ridge was rifting the Seychelles block from western India. Basalts from industry site SM-1 on the Saya de Malha Bank are 45 Ma old (Meyerhoft and Kamen-Kaye, 1981). On the

Nazareth Bank, basalts from the industry site NB-1 and ODP site 706 erupted 33 and 31 Ma, respectively (Duncan and Hargaves, 1990; O'Neill et al., 2003).
La Réunion and Mauritius islands show volcanic activity spanning in age 0-3 Ma and 0.03-8 Ma, respectively (Moore et al., 2011). This indicates a rather long period of simultaneous volcanic activity on the two islands. Such a regional volcanism during the last 3–5 Ma likely requires a complex melt distribution at depth, inconsistent with a single and punctual source of partial melting and of magma concentration (Barruol and Fontaine, 2013).
Even if the Mauritius Island does not show at present any active volcano, the existence of a deep magmatic source more or less quiescent cannot be excluded (Moore et al., 2011). Volcanism of Mauritius and the nearby La Réunion is probably fed by the same magmatic source, as demonstrated by the chemical features of the erupted lavas (Demange et al., 1989). These similarities lead to a possible comparison of the geothermal potential of the two islands. In La Réunion, some research projects carried out in the late 1980s found temperatures of approximately 200 °C at about 2100 m depth (Sanjuan et al., 2000).
In this paper, we present the results of recent geochemical and geophysical investigations aimed at the evaluation of geothermal resources of Mauritius. The geochemical survey was carried out to investigate the interaction with groundwater and the possible magmatic system. Geothermal investigations consisted in thermal logging in a gradient hole, specifically drilled for this study, and some water wells. Information on the thermal regime was considered as a fundamental clue for deciding on the opportunity to conduct further geothermal surveys in the island.

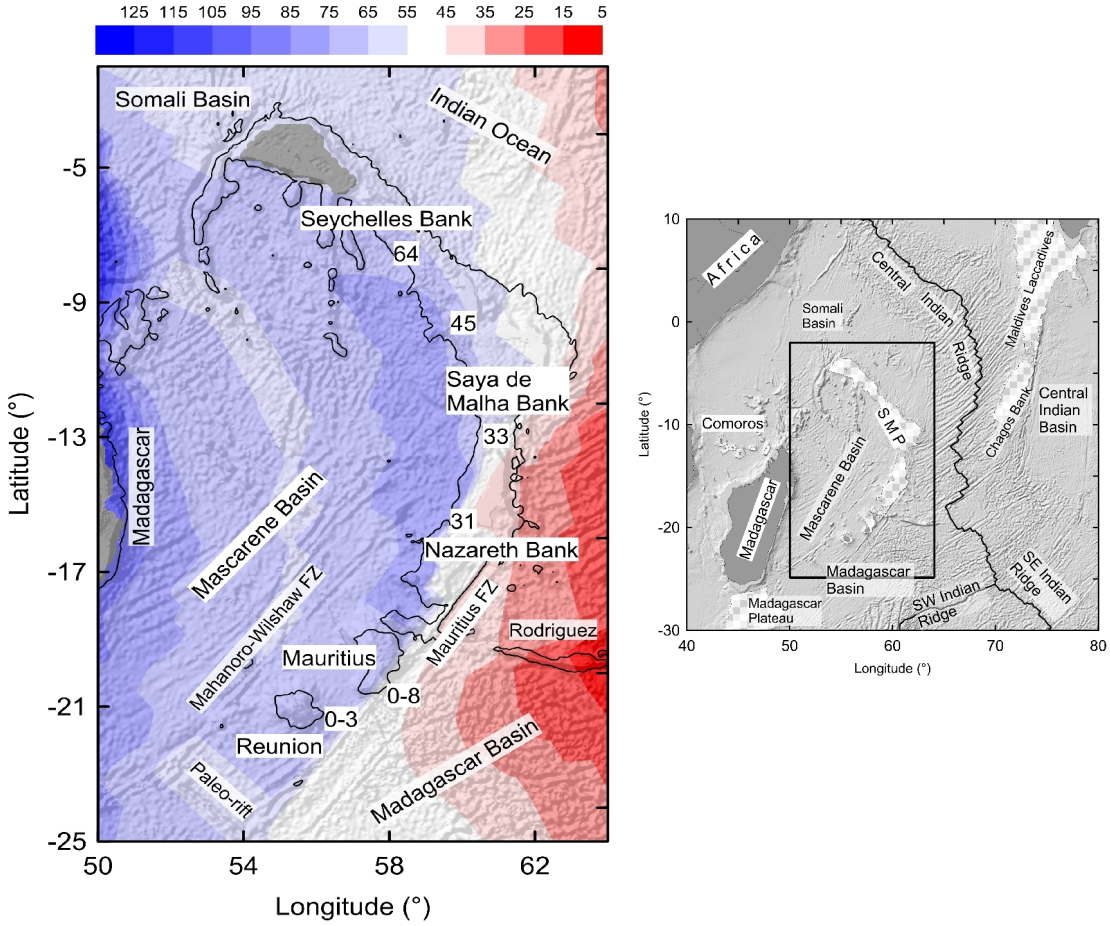


Figure 1: Position of the Seychelles-Mascarene plateau (SMP), superimposed on a map of seafloor age (colour scale in Ma) by Müller et al. (2008). Black line is the -2500 m observed topographic contour. White boxes show ages of hotspot volcanism (in Ma) after Duncan and Hargaves (1990) and Tiwari et al. (2007). Continental lithosphere in gray.

## 2. VOLCANO-TECTONIC SETTING

Mauritius corresponds to the minor dry land area of a typical, huge polygenic shield volcano, built on oceanic seafloor and has similar features to other hotspot related shield volcanoes in oceanic environment, like e.g. the Hawaiian volcanoes. Like any shield-type volcano, Mauritius is mostly made of lava flows. Volcanic type and overall morphology of Mauritius determine a general outward dipping of the main volcanostratigraphic discontinuities. This feature should be considered in any hydrogeological model.

The available volcanological data of Mauritius claim the presence of a caldera structure in the central part of the island (Paul et al., 2007). Indeed, this structure is hardly recognizable, as neither sharp counter-slopes, nor sub-circular depressions within a visible rim can be clearly identified in the topographic surface. In any case, the caldera should be pre-Quaternary in age and thus probably partly erased by recent morphogenetic processes. In contrast, a huge flank collapse, cutting the western side of the island, is deemed as very probable. Such catastrophic episode is considered as capable of triggering the volcanic rejuvenation after the last long-lasting activity hiatus.

Volcanism has developed on Mauritius during three phases, dated 7.8−5.5 Ma, 3.5−1.9 Ma, and 0.7−0.03 Ma, which are termed Older, Intermediate, and Younger Series, respectively (Paul et al., 2007; Moore et al., 2011 and references therein) (Fig. 2). The Older Series is subdivided into two stages: an early- and a late-shield building stage. Subaerially, the early-shield building stage is only visible in the erosional remnants of a single shield volcano that was built above sea level by the extrusion of transitional basalts (olivine basalt). Subsequent eruptions gave rise to the late-shield stage lavas and produced mainly hawaiites and mugearites with only small volumes of basalts and trachytes. After a 2 million year hiatus, renewed volcanism produced the olivine-phyric alkali basalts, basanites, and nephelinites of the Intermediate Series lavas. The Younger Series lavas are mostly olivine basalts with smaller volumes of basanites.

Similarly to La Réunion (see Michon et al., 2007), important fracture systems are observed, because of the combination of rigid rock types (i.e. basaltic lavas) and the geodynamic context, which is characterized by extensional to strike-slip tectonics and subsequent faulting and fracturing. All geodynamic models highlight a dense set of (probably deep-seated) fractures scattered around and between major fracture zones. In principle, this is considered as a regional-scale feature, which may produce high permeability conditions, i.e. favorable to potential geothermal resources (ELC, 2014).

Despite Mauritius volcano is considered still capable to erupt, the total absence of geothermal manifestations (such as steaming grounds, hot springs, etc.) seems to indicate that possible heat sources cannot be shallow magmatic chambers, but more likely may reside in deep-reaching fracture zones. This may hinder the interaction between the possible deep heat source and the infiltrating water.

All volcano-tectonic information point to the central part of Mauritius Island, in which the youngest volcanic events dated 0.03 Ma ago took place, as the most suitable to the assessment of the geothermal potential.

## 2. GEOCHEMICAL SURVEY

Twenty-nine water samples were collected from boreholes drilled at shallow depths for different purposes, including domestic, agricultural and industrial uses (Fig. 2). Chemical and isotopic analyses were performed and results are summarized in Table 1. Moreover, total dissolved inorganic carbon (TDIC), TDIC speciation, $CO_2$ partial pressure and saturation index (SI) with respect to calcite, computed by means of the speciation-saturation code EQ3 (Wolery and Jarek, 2003) were determined (Table 2). The geochemical data allowed (i) the definition of the water chemistry, (ii) the calculation of the speciation-saturation, identifying the distribution of $CO_2$ partial pressure, and the saturation index with respect to calcite, (iii) characterising the origin of groundwater, (iv) estimating the reservoir temperatures with water geothermometers.

Most of the collected samples are $HCO_3$ waters with in general comparable concentrations of Ca, Mg, and Na, low-salinity (2.1 to 9.6 meq/l), and low outlet temperature (23 to 29 °C) (Table 1). They are

originated through dissolution of local volcanic rocks, mainly those of the younger series, driven by conversion of aqueous $CO_2$ to $HCO_3$-ion.

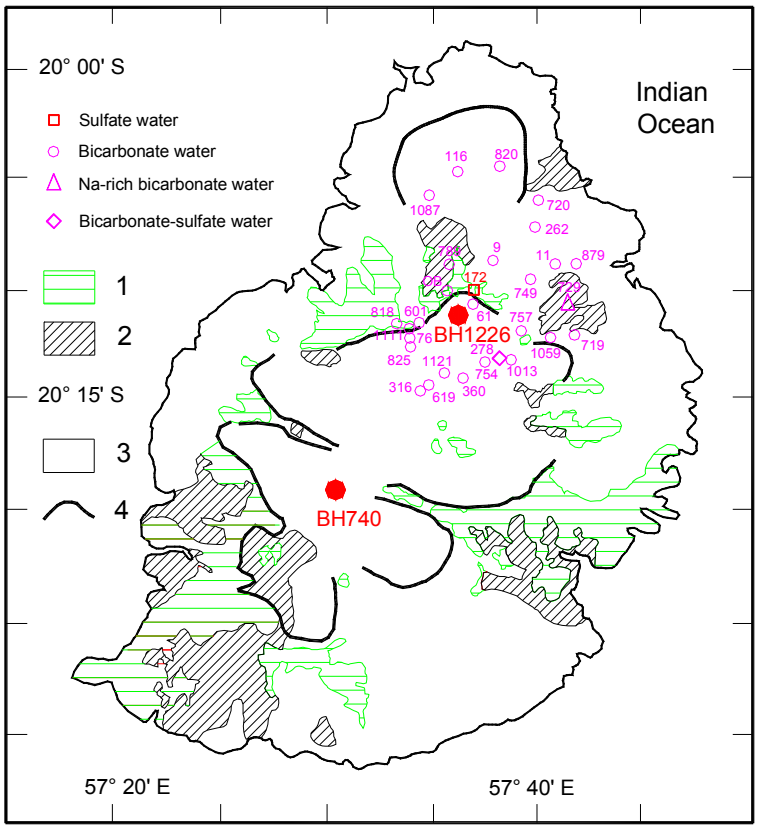


Figure 2: Location of the water samples from Mauritius and position of the gradient hole (BH1226) and the water well (BH740) used for thermal logging, superimposed on a geological sketch: volcanic series: (1) Older, (2) Intermediate, (3) Younger; (4) caldera limit.

The cumulative distribution of $CO_2$ partial pressure (Table 2) shows a population with lower values (0.0513-0.0108 bar), ascribable to decay of organic matter and root respiration in soils, and a population with larger values (0.1160-0.0564 bar), probably a mixture of shallow and deep contributions, rather than the expression of deep sources only. In any case, the involvement, even partial, of one or more deep $CO_2$ sources does not necessarily implies the presence of a geothermal system at shallow-intermediate depth. In fact, due to the very low solubility of $CO_2$ in magmas, the flux of deep $CO_2$ may result from magmatic degassing, occurring at great depth. There is general undersaturation with calcite indicating that all the water samples are immature, as the equilibrium with calcite is attained rather quickly due to the high dissolution rate of this mineral.

The $\delta D$ and $\delta^{18}O$ values of all the groundwater samples are within the ranges of the local rainwater, indicating a meteoric origin (Fig. 3). In addition, there is no oxygen isotope shift as it usually occurs in many geothermal waters (Giggenbach, 1991 and 1992).

Figure 4 shows the triangular Mg-K-Na diagram, differently scaled with respect to the original plot proposed by Giggenbach (1988) to shift the data points towards the center of the diagram. The condition expected for attainment of full equilibrium between the aqueous solution and the authigenic hydrothermal minerals produced by iso-chemical recrystallization of an average crustal rock is represented by the full equilibrium line, which is constrained by the Na-K geothermometer of Fournier (1979) and the K-Mg geothermometer of Giggenbach (1988).

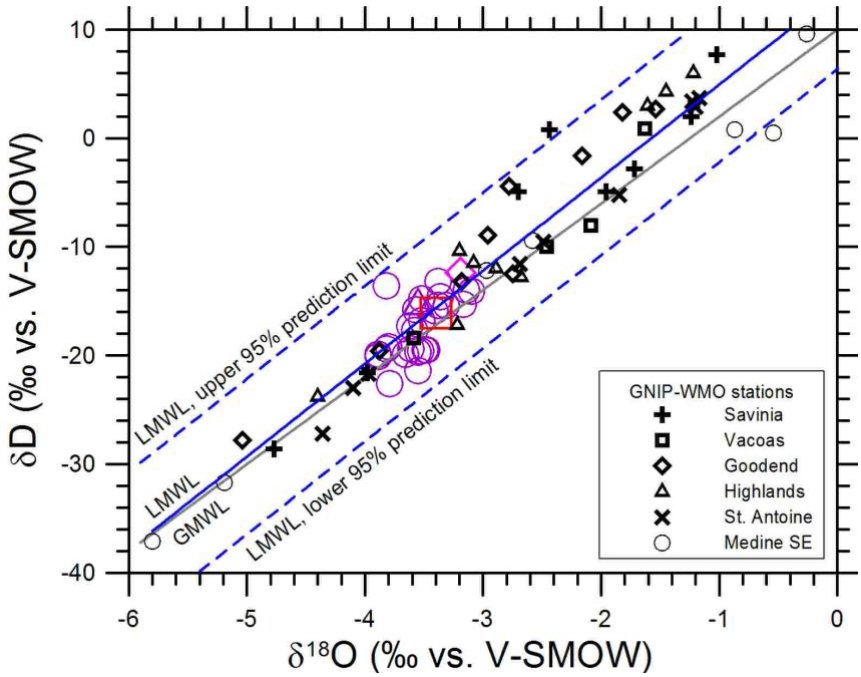


Figure 3: Plot of δD vs. $\delta^{18}O$ values of the groundwater samples from Mauritius (values in Table 1; color symbols as in Fig. 2). Monthly average data of rainwater from the stations positioned on Mauritius Island extracted from the database of the Global Network of Isotopes in Precipitation (GNIP) of the World Meteorological Organization (WMO) are also plotted (black symbols). The Global Meteoric Water Line (GMWL) and the Local Meteoric Water Line (LMWL), as well as the upper and lower 95% prediction limits of the LMWL are shown.

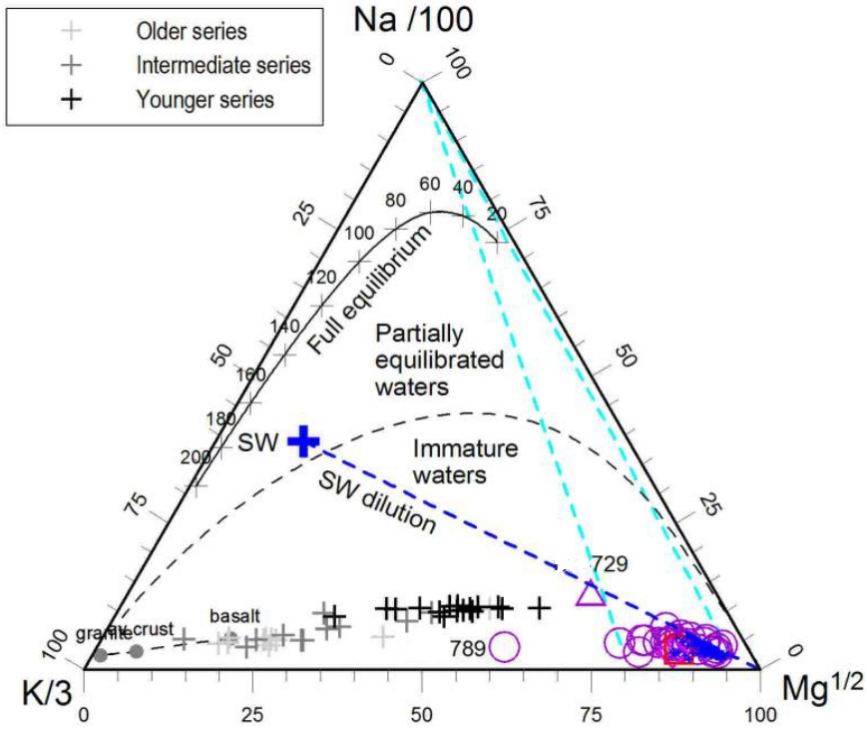


Figure 4: Triangular diagram of Na/100-K/3-$Mg^{1/2}$ for water samples of Mauritius (colour symbols like in Fig. Average seawater SW and dilution line (blue dashed line; from Nordstrom et al., 1979); rainwater samples (blue crosses) from stations VI01 of NADP/NTN, Virgin Islands (http://nadp.sws.uiuc.edu/nadpdata/ntnsites.asp). Compositions expected through dissolution of granite, basalt and an average crustal rock (gray dots), as well as of local volcanic rocks (gray crosses) (from Sheth et al., 2003 and Nohda et al., 2005) are also shown. Symbols of water samples like in Fig. 2. K-Mg geothermometer is indicated by the cyan dashed lines.

All the samples plot in the field of immature waters. The temperature of the aquifer of immature waters can be obtained by using the K-Mg geothermometer, provided that they are not too acidic (Giggenbach, 1988). Excluding samples 729 and 789 (as they are unusually rich in Na and K, respectively, due to ion exchange during freshening and anthropogenic pollution) and applying the K-Mg geothermometer (i.e., drawing a line connecting a given sample with the Na vertex), equilibrium temperatures of 5-36 °C are obtained. Although the meaningfulness of these temperatures is dubious, they do not deviate too much from outlet temperatures.

Table 1: Results of chemical and isotopical analyses on water samples. T – temperature; σ – electrical conductivity; VSMOW – Vienna Standard Mean Ocean Water

| Sample | T | pH | σ | Na | K | Mg | Ca | SO4 | Cl | SiO2 | Fe | $\delta^{18}O$ | δD |
|---|---|---|---|---|---|---|---|---|---|---|---|---|---|
| | °C | | µS cm$^{-1}$ | mg/l | mg/l | mg/l | mg/l | mg/l | mg/l | mg/l | mg/l | ‰ vs.VSMOW | |
| 316 | 25.8 | 6.25 | 207 | 10.7 | 0.57 | 9.7 | 15.9 | 4.99 | 8.76 | 18.3 | <0.005 | -3.14 | -14 |
| 619 | 24.9 | 6.43 | 203 | 10.3 | 0.56 | 9.08 | 15.4 | 4.63 | 9.53 | 18.9 | 0.011 | -3.36 | -14.6 |
| 757 | 25.9 | 6.63 | 168 | 12.3 | 0.81 | 6.38 | 11.4 | 4.31 | 10.2 | 12 | 0.047 | -3.41 | -15.9 |
| 1121 | 28.4 | 6.44 | 244 | 11.8 | 1.94 | 10 | 20.2 | 6.35 | 10.9 | 17.1 | 0.015 | -3.1 | -14.1 |
| 754 | 25.5 | 6.57 | 237 | 12.3 | 0.58 | 11.8 | 17.4 | 3.1 | 10.2 | 13.4 | <0.005 | -3.48 | -19.5 |
| 1013 | 27.2 | 6.91 | 273 | 12.5 | 0.64 | 16.1 | 17.6 | 4.27 | 11 | 18.2 | <0.005 | -3.38 | -15.4 |
| OB | 24.0 | 6.15 | 196 | 14 | 1.71 | 5.55 | 12.8 | 7.75 | 16.3 | 8.6 | 0.006 | -3.66 | -19.9 |
| 172 | 25.2 | 5.33 | 248 | 11.4 | 1.02 | 8.11 | 15.3 | 44.6 | 14.7 | 1.69 | 1.08 | -3.4 | -16.1 |
| 825 | 25.5 | 6.43 | 176 | 11.5 | 0.73 | 8.38 | 10.4 | 1.79 | 9.3 | 18.5 | 0.025 | -3.61 | -19.4 |
| 76 | 26.4 | 6.5 | 205 | 14.9 | 0.88 | 8.52 | 11.5 | 2.05 | 13.9 | 13.5 | 0.007 | -3.89 | -20.1 |
| 1111 | 26.3 | 6.56 | 163 | 12.6 | 0.97 | 6.41 | 10.8 | 2.84 | 9.79 | 13 | 0.032 | -3.82 | -13.6 |
| 601 | 24.6 | 6.21 | 118 | 8.34 | 0.32 | 4.32 | 8.74 | 3.72 | 10.7 | 5.53 | 0.22 | -3.57 | -15.8 |
| 61 | 23.1 | 6.57 | 114 | 10.4 | 0.89 | 2.7 | 6 | 2.85 | 11.3 | 6.79 | 0.161 | -3.55 | -21.4 |
| 789 | 27.2 | 6.77 | 377 | 20.5 | 5.61 | 9.85 | 20.3 | 5.27 | 21.7 | 30.9 | 0.031 | -3.38 | -13.2 |
| 9 | 25.8 | 6.22 | 195 | 15.6 | 0.6 | 8.86 | 6.14 | 8.47 | 19.4 | 15.5 | 0.007 | -3.58 | -17.7 |
| 1087 | 27.6 | 7.01 | 460 | 39 | 1.68 | 19.9 | 25.8 | 5.7 | 26.8 | 17.9 | <0.005 | -3.79 | -22.6 |
| 116 | 26.3 | 6.37 | 409 | 31.9 | 1.44 | 21.2 | 19.4 | 6.97 | 21.5 | 30.2 | 0.053 | -3.62 | -17.3 |
| 820 | 28.9 | 6.84 | 468 | 31.2 | 1.29 | 24 | 24.3 | 10.9 | 28 | 24.7 | 0.008 | -3.53 | -19.6 |
| 720 | 27.6 | 6.2 | 295 | 21.7 | 0.7 | 14.2 | 11.8 | 8.07 | 22.2 | 25.8 | 0.005 | -3.52 | -14.8 |
| 262 | 27.0 | 5.93 | 248 | 20.3 | 1.81 | 10.3 | 10.1 | 10.1 | 26.3 | 14.1 | 0.123 | -3.31 | -15.4 |
| 11 | 24.6 | 6.52 | 169 | 13.2 | 0.95 | 5.78 | 9.64 | 5.62 | 14.7 | 11 | 0.005 | -3.49 | -19.5 |
| 879 | 25.8 | 6.5 | 202 | 14.7 | 1.1 | 6.88 | 11.4 | 6.36 | 18.7 | 11.7 | 0.018 | -3.52 | -16.8 |
| 749 | 25.8 | 6.65 | 168 | 13.6 | 1.1 | 5.71 | 9.6 | 5.41 | 14.5 | 10.6 | 0.015 | -3.55 | -19.7 |
| 729 | 27.6 | 6.77 | 264 | 42.2 | 1.76 | 4.73 | 8.67 | 1.77 | 24 | 7.73 | 0.012 | -3.55 | -15 |
| 1059 | 26.5 | 6.28 | 211 | 14.5 | 0.37 | 10.4 | 11.4 | 6.38 | 14.3 | 15.7 | 0.013 | -3.17 | -15.3 |
| 719 | 26.2 | 6.48 | 200 | 14.3 | 1.05 | 9.33 | 11.8 | 2.44 | 11.3 | 14.7 | 0.014 | -3.8 | -19.2 |
| 818 | 23.7 | 6.07 | 177 | 14.1 | 1.28 | 11.4 | 17.9 | 1.94 | 10.1 | 9.35 | 0.055 | -3.89 | -19.9 |
| 360 | 24.0 | 6.76 | 240 | 14.7 | 0.86 | 5.6 | 11.7 | 5.02 | 18 | 12.4 | 0.027 | -3.82 | -19.4 |
| 278 | 25.1 | 6.53 | 207 | 11.4 | 1.35 | 11.3 | 14 | 22.2 | 14.9 | 14 | 0.029 | -3.19 | -12.4 |

In summary, there is no geochemical indication on the possible presence of a geothermal system at depth in the explored area of Mauritius Island and chemical features are ascribable to short-term water-rock interaction in shallow hydrological circuits. However, it cannot be ruled out that a deep heat source, hydraulically insulated from shallow aquifers, can occur.

## 4. GEOTHERMAL GRADIENT ASSESSMENT

A 270 m deep hole was drilled in the central part of the island for downhole temperature measurements and the evaluation of the geothermal gradient (Fig. 2). The hole BH1226 was drilled since May 2013 within the framework of the present project and was terminated on June 2014. The

well site is located at 416 m a.s.l. along the ENE flank of Bar Le Duc - L'Escalier polygenic volcano in the central part of the island and lies inside the rim of the inferred caldera structure.

Table 2: Total dissolved inorganic carbon (TDIC), TDIC speciation, partial pressure of $CO_2$ and saturation index SI with respect to calcite, for water samples from boreholes of Mauritius Island. Total alkalinity values reported in bold were measured in the field

| Sample | T °C | pH | Alkalinity | TDIC | TDIC | $HCO_3$ | $CO_2$ | $P_{CO2}$ | SI calcite |
|---|---|---|---|---|---|---|---|---|---|
| | | | mg $HCO_3$/l | mg $HCO_3$/l | mol/l | mol/l | mol/l | bar | |
| 316 | 25.8 | 6.25 | 99.6 | 214 | 3.51E-03 | 1.63E-03 | 1.87E-03 | 5.64E-02 | -1.90 |
| 619 | 24.9 | 6.43 | 93.5 | 165 | 2.70E-03 | 1.53E-03 | 1.18E-03 | 3.45E-02 | -1.80 |
| 757 | 25.9 | 6.63 | 75.2 | 111 | 1.82E-03 | 1.23E-03 | 5.94E-04 | 1.80E-02 | -1.80 |
| 1121 | 28.4 | 6.44 | 101.7 | 174 | 2.85E-03 | 1.66E-03 | 1.19E-03 | 3.86E-02 | -1.60 |
| 754 | 25.5 | 6.57 | 112.9 | 175 | 2.87E-03 | 1.84E-03 | 1.02E-03 | 3.03E-02 | -1.50 |
| 1013 | 27.2 | 6.91 | 146.4 | 182 | 2.98E-03 | 2.39E-03 | 5.85E-04 | 1.84E-02 | -1.10 |
| OB | 24.0 | 6.15 | 66.1 | 165 | 2.70E-03 | 1.08E-03 | 1.62E-03 | 4.62E-02 | -2.30 |
| 172 | 25.2 | 5.33 | 19.3 | 209 | 3.43E-03 | 3.20E-04 | 3.10E-03 | 9.17E-02 | -3.60 |
| 825 | 25.5 | 6.43 | 91.5 | 162 | 2.65E-03 | 1.50E-03 | 1.15E-03 | 3.43E-02 | -2.00 |
| 76 | 26.4 | 6.50 | 98.6 | 162 | 2.65E-03 | 1.61E-03 | 1.04E-03 | 3.19E-02 | -1.80 |
| 1111 | 26.3 | 6.56 | **81.4** | 127 | 2.08E-03 | 1.33E-03 | 7.52E-04 | 2.30E-02 | -1.80 |
| 601 | 24.6 | 6.21 | **48.8** | 112 | 1.84E-03 | 7.99E-04 | 1.04E-03 | 3.03E-02 | -2.50 |
| 61 | 23.1 | 6.57 | 40.7 | 64.5 | 1.06E-03 | 6.66E-04 | 3.90E-04 | 1.08E-02 | -2.40 |
| 789 | 27.2 | 6.77 | **150.5** | 201 | 3.29E-03 | 2.45E-03 | 8.31E-04 | 2.61E-02 | -1.10 |
| 9 | 25.8 | 6.22 | **44.7** | 100 | 1.64E-03 | 7.32E-04 | 9.10E-04 | 2.74E-02 | -2.70 |
| 1087 | 27.6 | 7.01 | **248.1** | 295 | 4.83E-03 | 4.04E-03 | 7.69E-04 | 2.44E-02 | -0.59 |
| 116 | 26.3 | 6.37 | **191.2** | 353 | 5.79E-03 | 3.12E-03 | 2.65E-03 | 8.10E-02 | -1.50 |
| 820 | 28.9 | 6.84 | **199.3** | 254 | 4.16E-03 | 3.25E-03 | 9.00E-04 | 2.96E-02 | -0.86 |
| 720 | 27.6 | 6.20 | **97.6** | 220 | 3.61E-03 | 1.60E-03 | 2.00E-03 | 6.36E-02 | -2.10 |
| 262 | 27.0 | 5.93 | **65.1** | 219 | 3.59E-03 | 1.07E-03 | 2.52E-03 | 7.88E-02 | -2.60 |
| 11 | 24.6 | 6.52 | 53.9 | 88.1 | 1.44E-03 | 8.81E-04 | 5.60E-04 | 1.63E-02 | -2.10 |
| 879 | 25.8 | 6.50 | 69.1 | 114 | 1.87E-03 | 1.13E-03 | 7.36E-04 | 2.22E-02 | -2.00 |
| 749 | 25.8 | 6.65 | 52.9 | 77.3 | 1.27E-03 | 8.65E-04 | 4.01E-04 | 1.21E-02 | -2.00 |
| 729 | 27.6 | 6.77 | 121.0 | 162 | 2.65E-03 | 1.98E-03 | 6.73E-04 | 2.14E-02 | -1.60 |
| 1059 | 26.5 | 6.28 | 95.6 | 197 | 3.23E-03 | 1.56E-03 | 1.67E-03 | 5.13E-02 | -2.00 |
| 719 | 26.2 | 6.48 | 105.7 | 177 | 2.90E-03 | 1.73E-03 | 1.17E-03 | 3.56E-02 | -1.80 |
| 818 | 23.7 | 6.07 | 140.3 | 390 | 6.39E-03 | 2.29E-03 | 4.09E-03 | 1.16E-01 | -1.90 |
| 360 | 24.0 | 6.76 | 63.0 | 86.1 | 1.41E-03 | 1.03E-03 | 3.79E-04 | 1.08E-02 | -1.70 |
| 278 | 25.1 | 6.53 | 81.3 | 131 | 2.15E-03 | 1.33E-03 | 8.09E-04 | 2.39E-02 | -1.80 |

A drilling depth of 500 m was initially planned for BH1226. This depth was suggested to avoid possible influences of shallow, cold aquifers on the measured temperatures and to provide reliable information of the true deep thermal gradient. Actually, several water strikes at different depths were noticed during drilling. Water inflows occurred at about 60 m, 120 m and 180 m depth. Unfortunately, due to technical problems encountered while drilling the target depth of the gradient well was not achieved. Drilling stopped at 432 m bsl and casing was inserted only to about 270 m depth.

From the lithological viewpoint, the hole encountered a sequence of basaltic lava flows and pyroclastic deposits, belonging to the three chronologically distinct magmatic cycles (Older, Intermediate and Younger Series), with thin intercalations of laterite which was considered as a marker of the main volcanic cycles (Fig. 5).

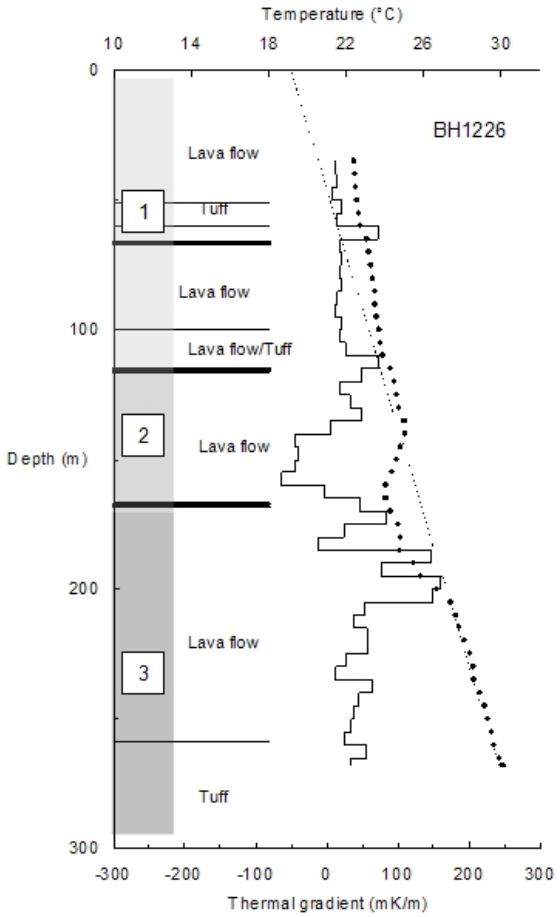


Figure 5: Temperature (dots), thermal gradient versus depth (step line) and stratigraphy of the borehole BH1226. (1) Older, (2) Intermediate, (3) Younger volcanic Series. Bold line marks the lateritic levels. Dashed line indicates the least square linear regression.

Down-hole temperature logs were carried out in the 270 m cased section of the hole. Temperature was recorded at 5-m depth intervals by means of a precision temperature acquisition system with an uncertainty of ~ 0.01 K (see Verdoya et al. 2008 for equipment details). Thermal log shows significant perturbation due to groundwater flow, especially between 150 and 210 m, which causes distortion of the temperature depth profile and therefore biases the inference of the geothermal gradient in the upper section of the hole. Actually, it is observed that thermal gradient is negative at shallow depth (30-40 m), then it is relatively constant between 40 and 110 m; in the interval 110-210 m the largest variations of gradient, often turning to negative, occur, whereas below this depth the gradient appears to be quite constant.

The deeper level appears to be in a purely conductive thermal regime with an estimated thermal gradient of 43 °C $km^{-1}$. By extrapolating such gradient downwards, a temperature of 180 °C (a possible target temperature for geothermal exploitation) can be expected at a depth of about 4000 m.

Comparative measurements were also made in a water well (BH740, Fig. 2) 10 km far from BH1226, no longer used for extraction. The well is 170 m deep and has the water table at 13 m b.g.l. As shown in Fig. 6, a null gradient was recorded up to 95 m, followed by a gradient of 20-40 °C $km^{-1}$ in the 95-115 m interval, which is consistent with the conductive gradient inferred in the deepest part of BH1226. Below this level gradient turns again to null or negative and increases again in the last twenty meters. Such thermal gradient distribution can be interpreted as due to the presence of thin impermeable layers sandwiched between pervious horizons where intense groundwater circulation is taking place.

In conclusion, thermal measurements indicate the absence of a significant thermal anomaly in the sector of Mauritius singled out as the most favorable for geothermal resources.

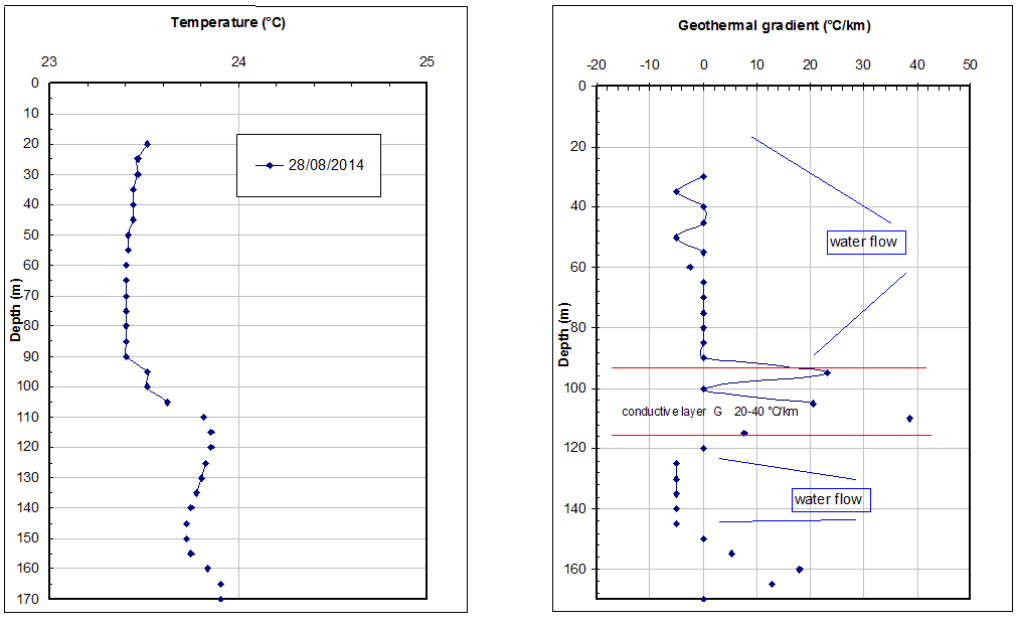


Figure 6: Temperature and thermal gradient G vs. depth in well BH740.

## 5. CONCLUDING REMARKS

The Mauritius Island is characterized by intense and recent tectonic activity, which produced widespread fracturing and hence adequate permeability of the lavic formations. All available geological information indicated that the central part of the island is the most favorable to host a geothermal system. However, chemical characters of water samples collected in wells show only short-term water-rock interactions in shallow hydrological circuits.

The down-hole temperature logs run in a gradient hole yielded a thermal gradient of 43 °C km$^{-1}$. Such a value exceeds by only about 1.3 times the "normal" geothermal gradient. Another attempt of assessing the geothermal gradient in a water well drilled in the same area confirmed the presence of a weak or null deep-seated thermal anomaly beneath Mauritius Island.

Although Mauritius volcanism was active until 0.03 My ago, the comparison of the geothermal gradient from offshore measurements in the Mascarene Plateau shows that the gradient measured in Mauritius is even lower than that observed in the 60-80 My old oceanic lithosphere (Chiozzi et al., 2015). This might mean that the deep thermal processes (mantle plume) invoked to occur in the Mascarene hotspot area do not likely yield any particular thermal signature.

Temperature logging in La Réunion Island revealed a geothermal gradient relatively larger than Mauritius, which however exceeds by only 1.7-2.8 times the world average (Demange et al., 1989). Moderate thermal anomalies seem a common feature in the geological environment of Ocean Islands. Geothermal heat sources in basaltic volcanoes of ocean islands (hotspot areas) rely on frequent but small eruptions. In contrast, along convergent plate boundaries and on the continents, eruptions are less frequent, but heat sources are shallow and large (Wohletz and Grant, 1992). Therefore, in spite of the still present volcanic activity, it is not surprising that moderate thermal anomalies were found in La Réunion. This strengthens the observation that the geothermal gradient of Mauritius, in which active volcanism is even lacking, is only slightly larger than normal one and thus consistent with the volcanic evolution and migration of the Mascarene hotspot.

## REFERENCES

Barruol, G. and Fontaine, F.R.: Mantle flow beneath Reunion hotspot track from SKS splitting, *Earth and Planetary Science Letters* 362, (2013), 108–121.

Chiozzi, P., Verdoya, M. and Pasqua, C.: New heat-flow observations in a hotspot swell: the Reunion-Mascarene Plateau, IUGG XXVI General Assembly, Prague 22 June -2 July (2015).

Demange, J. Chovelon, P., and Puvilland, P.: Geothermal model of the Salazie Cirque (Reunion Island): volcanic and structural implications, *J Volc Geoth Res* 36, (1989), 153–176.

Duncan, R.A. and Hargaves, R.B. 40 Ar/39 Ar geochoronology of basement rocks from the Mascrene plateau, the Chagos Bank and the Maldives Ridge. *Proceedings* Ocean Drill Program Sci Results 115, (1990), 43–51.

Duncan, R.A. and Richards, M.A.: Hotspots, mantle plumes, flood basalts, and true polar wander, *Rev Geophys* 29, (1991), 31–50.

Duncan, R.A., Backman, J. and McDonald, A.: Reunion hotspot activity through Tertiary time: Initial results from Ocean Drilling Program Leg 115, *J Volcanol Geotherm Res* 36, (1989), 193–198.

ELC Electroconsult: Opportunity assessment for the development of geothermal energy in Mauritius - Final Report, Ministry of Energy and Public Utilities of the Republic of Mauritius, (2014) 17 p. (unpublished report).

Fournier, R.O.: A revised equation for the Na/K geothermometer, *Geotherm. Res. Counc. Trans*., 5, (1979), 1-16.

Giggenbach, W.F.: Geothermal solute equilibria. Derivation of Na-K-Mg-Ca geoindicators, *Geochim. Cosmochim. Acta,* 52, (1988) 2749-2765.

Giggenbach, W.F.: Isotopic composition of geothermal water and steam discharges. In *Application of Geochemistry in Geothermal Reservoir Development*. (F. D'Amore, co-ordinator), UNITAR, (1991) 253-273.

Giggenbach, W.F.: Isotopic shifts in waters from geothermal and volcanic systems along convergent plate boundaries and their origin, *Earth Planet. Sci. Lett.* 113, (1992), 495-510.

Hammond, J.O.S., Collier, J.S., Kendall, J.M., Helffrich, G. and Rumpker, G.: Plume scar in the mantle lithosphere beneath the Seychelles revealed by seismic imaging, *Earth Planet Sci Lett* 355–356, (2012), 20–31.

Meyerhoff, A.A. and Kamen-Kaye, M.: Petroleum prospects of the Saya de Malha and Nazareth banks, Indian Ocean, *AAPG Bull* 65 (1981), 1344–1347.

Michon, L., Saint-Ange F., Bachelery, P., Villeneuve, N. and Staudacher, T.: Role of the structural inheritance of the oceanic lithosphere in the magmato-tectonic evolution of Piton de la Fournaise volcano (La Réunion Island), *J Geophys Res* 112, (2007) B04205, doi:10.1029/2006JB004598.

Moore, J., White, W.M., Paul, D., Duncan, R.A., Abouchami, W. and Galer, S.J.G.: Evolution of shield-building and rejuvenescent volcanism of Mauritius, *J Volc Geoth Res*, 207 (2011), 47–66.

Müller RD, Sdrolias M, Gaina C, Roest W Age, spreading rates, and spreading asymmetry of the world's ocean crust, Geochem Geophys Geosys 9, (2008) Q04006, http://dx.doi.org/10.1029/2007GC001743.

Nohda, S., Kaneaoka, I., Hanyut, T., Xu, S. and Uto, K.: Systematic variation of Sr-, Nd- and Pb-isotopes with time in lavas of Mauritius, Réunion hotspot, *J. Petrol*, 46, (2005), 505-522.

Nordstrom, D.K., Plummer, L.N., Wigley, T.M.L., Wolery, T.J., Ball, J.W., Jenne, E.A., Bassett, R.L., Crear, D.A., Florence, T.M., Fritz, B., Hoffman, M., Holdren, G.R. jr., Lafon, G.M., Mattigod, S.V., McDuff, R.E., Morel, F., Reddy, M.M., Sposito, G. and Thrailkill J.: A comparison of computerized chemical models for equilibrium calculations in aqueous systems, In: E.A. Jenne (Ed.), *Chemical Modeling in Aqueous Systems*, American Chemical Society Symposium Series, 93, (1979), 857-892.

O'Neill, C., Müller, R.D. and Steinberger, B.: Geodynamic implications of moving Indian Ocean hotspots, *Earth Planet Sci Lett*, 215, (2003), 151–168.

Paul, D., Kamenetsky V.S., Hofmann, A.W. and Stracke A.: Compositional diversity among primitive lavas of Mauritius,Indian Ocean: Implications for mantle sources, *Journal of Volcanology and Geothermal Research* 164, (2007), 76–94.

Sanjuan, B., Traineau, H., Rançon, J.Ph., Rocher, Ph. and Demange, J.: Le potential géothermique de l'île del Reunion. Bilan des connaissances et perspectives, Rapport BRGM / RP-50388-FR-2000 SGR/REU 31, (2000), 89 pp.

Sheth, H.C., Mahoney, J.J. and Baxter, A.N.: Geochemistry of lavas from Mauritius, Indian Ocean: mantle sources and petrogenesis, *Int. Geology Review*, 45, (2003), 780–797.

Tiwari, V.M., Grevemeyer, I., Singh, B. and Phipps Morgan, J.: Variation of effective elastic thickness and melt production along the Deccan-Reunion hotspot track, *Earth Planet Sci Lett* 264, (2007), 9–21.

Verdoya, M., Pasquale, V. and Chiozzi, P.: Inferring hydro-geothermal parameters from advectively perturbed thermal logs, *Int J Earth Sci (Geol Rundsch),* 97, (2008), 333–344.

Wohletz, K. and Grant, H.: Volcanology and Geothermal Energy. Berkeley, University of California Press, (1992), http://ark.cdlib.org/ark:/13030/ft6v19p151/

Wolery, T.W. and Jarek, R.L.: Software user's manual. EQ3/6, Version 8.0. Sandia National Laboratories – U.S. Dept. of Energy Report (2003).